Structural and spectroscopic characterisation of C4 oxygenates relevant to structure/activity relationships of the hydrogenation of α,β-unsaturated carbonyls

Ian P. Silverwood,[1] Neil G. Hamilton,[1] David Lennon[1] and Stewart F. Parker,[2]*

1. School of Chemistry, Joseph Black Building, University of Glasgow, Glasgow G12 8QQ, Scotland, UK.

2. ISIS Facility, STFC Rutherford Appleton Laboratory, Chilton, Didcot, Oxon OX11 0QX, UK.

*Corresponding author. Tel.: +44 1235 446182.

E-mail address: stewart.parker@stfc.ac.uk

Abstract

Supported palladium catalysts are widely used in selective hydrogenation reactions, thus it is desirable to correlate product yields with catalyst performance, so as to optimize catalyst productivity. One method to achieve this goal is to use gas phase infrared spectroscopy to follow the evolution of the gas phase composition as a catalytic reaction progresses and hence determine the kinetics of the reaction. The method is critically dependent on reliable identification and assignment of the modes of each of the species that may be present. We plan to use the same method to investigate how the morphology of Pd crystallites can influence selectivity branching in gas phase hydrogenation reactions of α,β-unsaturated carbonyl compounds, specifically by following the hydrogenation of 3-butyne-2-one to 3-butene-2-one to 2-butanone and finally to 2-butanol. In the present work, we have investigated the conformational isomerism and calculated the vibrational spectra of the C4 oxygenates using density functional theory. The calculations are validated by comparison to the inelastic neutron scattering and infrared spectra of the compounds.

Keywords

Highlights

- The conformational isomerism in 3-butyne-2-one, 3-butene-2-one, 2-butanone and 2-butanol oxygenates has been investigated.

- Complete vibrational assignments for 3-butyne-2-one, 3-butene-2-one, 2-butanone and 2-butanol are obtained from density functional theory.

- The assignments have been tested by comparison to inelastic neutron scattering spectra.

Graphical abstract
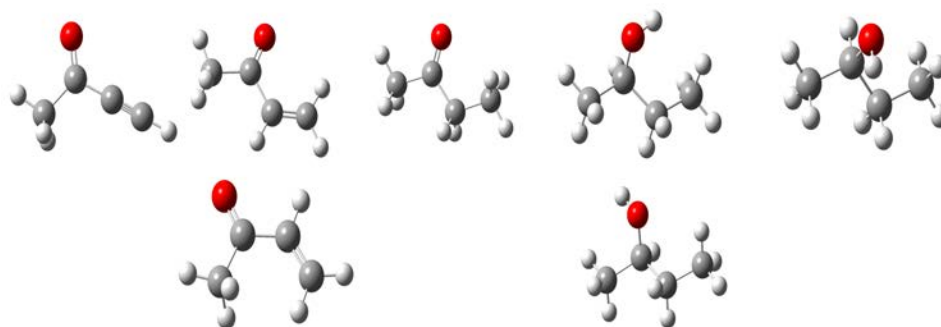
1. **Introduction**

Heterogeneous catalysis is an activity where there is a relentless drive to improve outcomes. One way this is achieved is to define structure/activity relationships for specified reactions [1,2] Supported palladium catalysts are widely used in selective hydrogenation reactions [3-5], thus it is desirable to correlate product yields with catalyst performance, so as to optimize catalyst productivity.

One method to achieve this goal is to use gas phase infrared spectroscopy to follow the evolution of the gas phase composition as a catalytic reaction progresses and hence determine the kinetics of the reaction. The hydrogenation of unsaturated species is a process that is conveniently followed by this method and was used to study the hydrogenation of C5 dienes [6,7]. The method is critically dependent on reliable identification and assignment of the modes of each of the species that may be present. For the C5 species considered in our previous work, we found that many of the species had only been poorly characterised, if at all, hence we undertook to comprehensively assign the spectra [8].

We plan to use the same method to investigate how the morphology of Pd crystallites can influence selectivity branching in gas phase hydrogenation reactions of α,β-unsaturated carbonyl compounds, specifically the hydrogenation of 3-butyne-2-one as shown schematically in Figure 1. The aim of this paper is to provide a complete assignment of the internal modes of the compounds studied: 3-butyne-2-one, 3-butene-2-one, 2-butanone and 2-butanol, (see Figure 2).
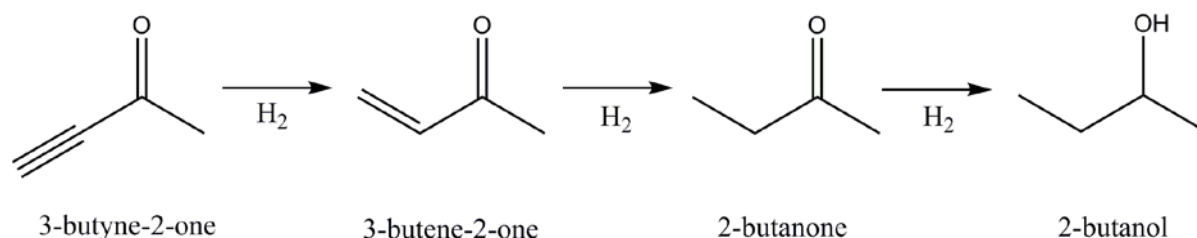

Figure 1. A reaction scheme for the hydrogenation of 3-butyne-2-one to 2-butanol *via* 3-butene-2-one and 2-butanone.

In the present work, we have calculated the spectra using density functional theory (DFT) of the gas phase (*i.e.* isolated) molecule. The calculations are validated by comparison to the inelastic neutron scattering (INS) spectra [9] of these compounds. Since these are obtained in the solid state, periodic-DFT calculations of the complete unit cell would appear to be more appropriate. These have not been carried out for two reasons: the crystal structure is not known for any of the compounds and the aim is to derive assignments for the gas phase species. In practice, as shown on many occasions previously [8-14], isolated molecule calculations give reasonable results for INS spectra, provided that the intermolecular interactions are weak. In the present case, this is only potentially a problem with 2-butanol and this will be considered later.
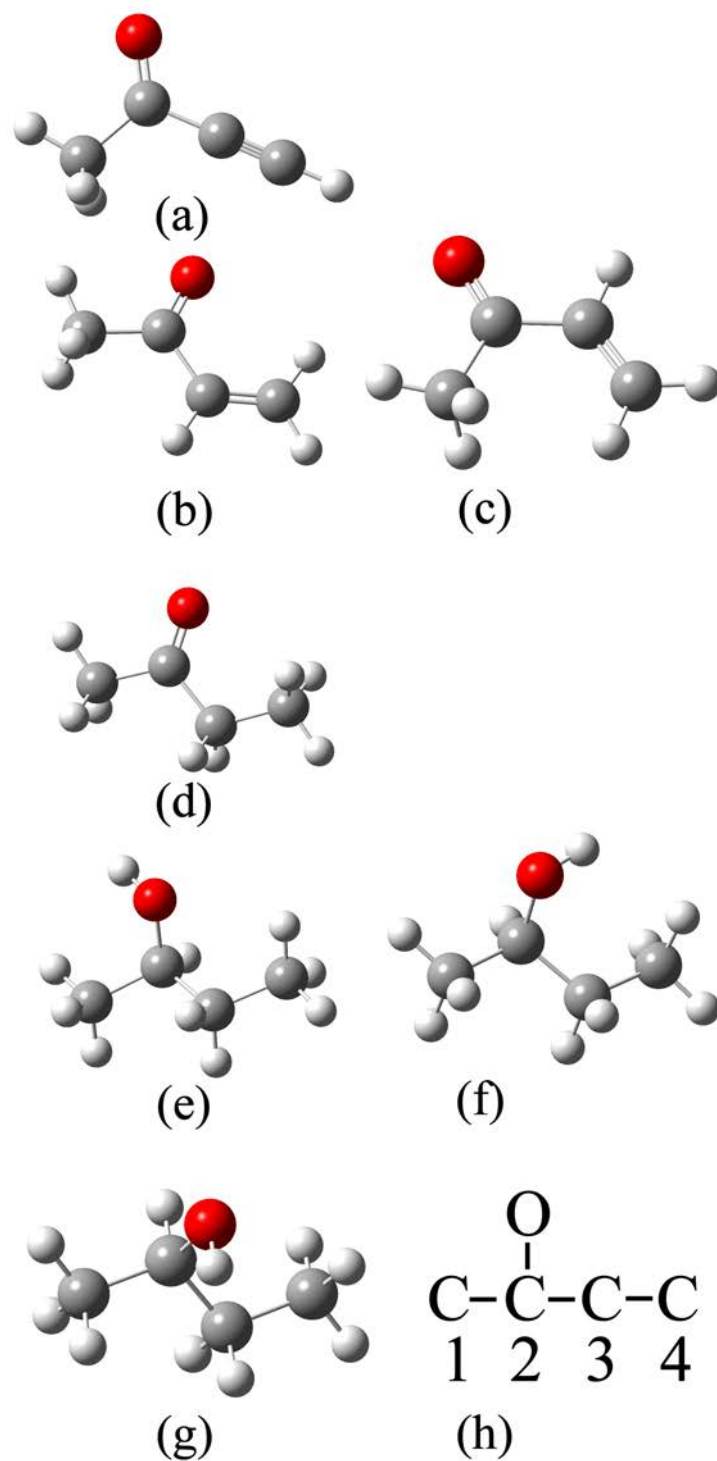
Figure 2. Chemical structures and conformations of the C4 species considered in this work (the point group is given in square brackets). (a) 3-Butyne-2-one (**1**) [C_s], (b) 3-butene-2-one *s-trans* conformer (**2**) [C_s], (c) 3-butene-2-one *s-cis* conformer (**3**) [C_s], (d) 2-butanone (**4**) [C_1], (e) 2-butanol conformer 1 (**5**) [C_1], (f) 2-butanol conformer 2(**6**), [C_1] (g) 2-butanol conformer 3 (**7**) [C_1] and (h) numbering system for the C4 species considered here..

2. Experimental

INS spectra [9] were recorded using TOSCA [15] at ISIS [16]. TOSCA has high resolution, ∼1.25% ΔE/E between 25 and 4000 cm^{-1}. The compounds were loaded into flat-plate aluminium cells sealed with indium gaskets, loaded into the spectrometer, cooled to ∼20 K and the spectra recorded for 3 - 6 hours. The INS spectra are available from the INS database at: http://wwwisis2.isis.rl.ac.uk/INSdatabase/.

Gas phase infrared spectra of the pure compounds were recorded from ~5 μL of sample at room temperature using a Graseby-Specac 5660 heated 10 cm pathlength gas cell fitted with KBr windows and a 20140 automatic temperature controller in a Nicolet Avatar 360 FTIR spectrometer.

DFT calculations of the geometry and vibrational transition energies were carried out using Gaussian 03 [17] with the B3LYP functional and AUG-cc-pVTZ basis set. Relaxed potential energy scans to locate conformers were carried out with the same functional and the 6-311g** basis set, in order to reduce the computation time required. Relative energies (the lowest energy conformer is used as the zero of energy) of conformers quoted in the text are corrected for zero point energy (ZPE), the figures showing relative energy are not corrected for ZPE. Mode visualisation of the results was realised with GaussView 3.09. The calculated INS spectra were generated from the Gaussian 03 output using the programme ACLIMAX [18].

3. Results and Discussion

For each of the molecules considered, we will present a comparison of observed and calculated structure and spectra and a table of assignments. Potential energy scans (PES) of relevant coordinates are carried out in cases where conformational isomerism is possible. Figure 2a – 2g shows the structures and conformations of all the species considered in this work, Figure 2h shows the numbering scheme for the carbon skeleton, in all cases the methyl group adjacent to the carbon bearing the oxygen atom is C1.

3.1   3-Butyne-2-one

Column 2 of Table 1 gives the calculated experimental structural data for 3-butyne-2-one, we are unaware of any experimental data for either the gas or condensed phases. Ignoring, the effect of the methyl group, (which we show later is negligible), there is only one possible conformer, which has C_s symmetry. Gas phase infrared and Raman and infrared spectra of the liquid have been reported [19], the liquid phase spectra show evidence for considerable hydrogen-bonding between the alkynic hydrogen and the carbonyl moiety. Our infrared gas phase spectrum is in good agreement with the literature. Comparisons of the observed and calculated infrared and INS spectra are shown in Figures 3 and 4 respectively. Table 2 lists the transition energies and assignments by DFT. The assignments are largely in agreement with those of Crowder [19] except for the methyl torsion which occurs at lower energy than previously assigned.

Table 1. Selected structural parameters for (**1** - **4**). Experimental values in brackets.

	3-Butyne-2-one C_s (**1**)	3-Butene-2-one C_s (*s-trans*) (**2**)	3-Butene-2-one C_s (*s-cis*) (**3**)	2-Butanone C_s (**4**)
Bond distance / Å				
C1–C2	1.508	1.514 (1.48)†	1.520 (1.504) †	1.515 (1.518)‡
C2–C3	1.456	1.485 (1.492)	1.492 (1.475)	1.520 (1.518)
C3–C4	1.201	1.331 (1.340)	1.342 (1.333)	1.522 (1.531)
C2–O	1.212	1.217 (1.24)	1.227	1.210 (1.218)
C1–H	1.087, 2 × 1.092	1.086, 2 × 1.091	1.091 2 × 1.096	1.087, 2 × 1.092 (1.102)
C2–H				2 × 1.095 (1.102)
C3–H		1.083	1.089	2 × 1.095 (1.102)

C4–H	1.062	2 × 1.082	2 × 1.087	3 ×1.090 (1.102)
Bond angle / °				
C1–C2–C3	115.8	119.5 (121)	119.6 (118)	116.3
C2–C3–C4	179.6	125.4 (123)	125.4 (122)	114.3 (113.4)
C1–C2–O	123.3	121.2 (123)	121.2 (115.6)	121.6 (122.5)
C3–C2–O	120.9	119.3 (116)	119.3 (115.6)	122.1 (121.3)
Dihedral angle / °				
C1–C2–C3–C4	0.0	0.0	180.0	2.2 (0.0)
C1–C2(–O)–C3	0.0	0.0	0.0	0.0
Rotational constants / MHz				
A	10277	8972 (8941)	10471 (10239)	9584 (9545)[*]

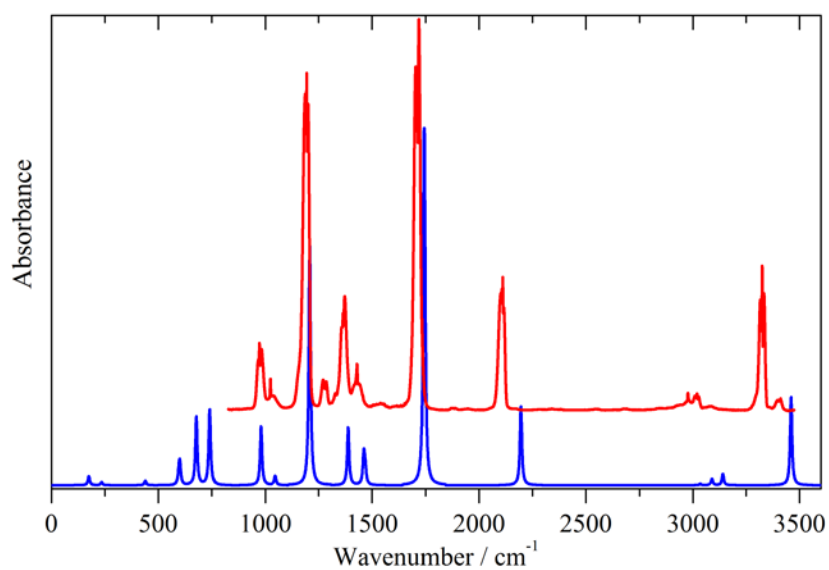|				
B	4048	4278 (4274)	3842 (3992)	3582 (3597)
C	2957	2950 (2945)	2861 (2925)	2739 (2747)

† Ref [24]

‡ Ref [31]

*Ref [32]

Figure 3. Comparison of measured (red, upper) and calculated (blue, lower) infrared spectra of 3-butyne-2-one (**1**).
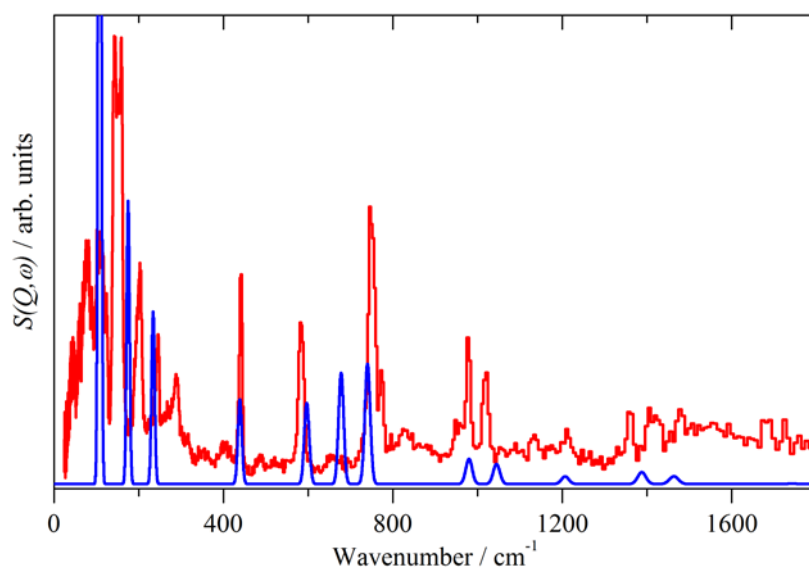

Figure 4. Comparison of measured (red, upper) and calculated (blue, lower) INS spectra of 3-butyne-2-one (**1**). Fundamentals only.

Table 2. Measured and calculated vibrational transition energies for 3-butyne-2-one.

Experimental / cm^{-1}		DFT			
Infrared (gas phase RT)	INS (solid 20 K)	/ cm^{-1}	Infrared intensity / km mol^{-1}	Symmetry	Assignment
	143,159 vs	108	0.02	A''	C1 methyl torsion
	204 s,br	175	5.31	A'	C2–C3–C4 in-plane bend
	246 m	234	1.76	A''	C2–C3–C4 out-of-plane bend
	440 s	439	2.60	A'	C1–C2–C3 in-plane bend
	584 s	597	5.3	A''	C=O out-of-plane bend
		601	12.04	A'	C=O in-plane bend
	745 s	678	40.50	A'	≡C–H in-plane bend
	745 s	740	32.04	A''	≡C–H out-of-plane bend
	774 w	742	13.86	A'	In-phase C–C stretches (C1–C2, C2–C3)
976 m	978 m	980	34.84	A'	Methyl rock
1024 w	1020 m	1046	5.41	A''	Methyl rock

1194 vs	1214 w	1207	143.60	*A′*	Out-of-phase C–C stretches (C1–C2, C2–C3)
1363 m	1360 w	1388	34.11	*A′*	Symmetric methyl HCH bend
1431 w	1416 w,br	1461	18.20	*A′*	Asymmetric methyl HCH bend
		1467	9.32	*A″*	Asymmetric methyl HCH bend
1715 vs		1744	211.38	*A′*	C=O stretch
2111		2196	46.62	*A′*	C≡C stretch
		3034	0.08	*A′*	Symmetric methyl stretch
2976 w		3089	3.66	*A″*	Asymmetric methyl stretch
3020 w		3140	6.62	*A″*	Asymmetric methyl stretch
3326 vs		3460	52.20	*A′*	≡C–H stretch

†s = strong; m = medium; w = weak; sh = shoulder; br = broad; v = very

3.2 3-Butene-2-one (methyl vinyl ketone)

3-Butene-2-one (methyl vinyl ketone, MVK) is the simplest α,β-unsaturated ketone and has attracted attention because it is important in atmospheric chemistry as a primary product of isoprene oxidation [20]. It has been studied in the gas phase by microwave spectroscopy [21-24] and by vibrational spectroscopy in all three phases [25-28] and also in an argon matrix [29]. There is general agreement that the molecule exists in two conformers, *s-trans* (**2**) and *s-cis* (**3**) and a potential energy scan around the C2–C3 bond confirms this as shown in Figure 5. The horizontal dashed line corresponds to kT = 373 K, the experimental reaction temperature and it can be seen that the barrier between the conformers is much larger than the available energy, thus both conformers will be present in the gas phase.
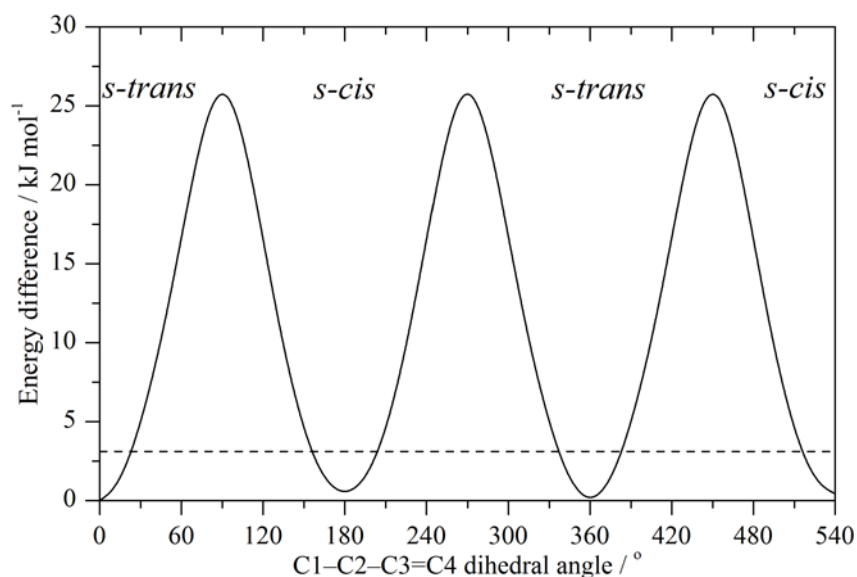

Figure 5. Potential energy scan around the C2–C3 bond of 3-butene-2-one. The horizontal dashed line corresponds to kT = 373 K, the experimental reaction temperature.

Columns 3 and 4 of Table 1 compare the calculated structures of the two conformers with the most recent microwave results [24]. The observed and calculated transition energies for the two conformers are given in Table 3 and comparisons of the infrared and INS spectra in Figures 6 and 7 respectively. The presence of two conformers is clearly seen in the infrared spectra, in particular the C=C stretch of the *s-cis* conformer at 1626 cm^{-1} is diagnostic as are the bands at 1182 and 1244 cm^{-1} assigned to the C–C stretching modes in (**3**) and (**2**) respectively. The two conformers have very different spectra in the low energy region and the calculated INS spectra, Figure 7, highlight these differences. The INS spectrum indicates that the solid is predominantly the *s-trans* conformer. The calculations were carried out using the same level of theory as Sankaran and Lee [29], thus our assignments are the same as theirs and also largely in agreement with the empirical assignments of Durig and Little [27].
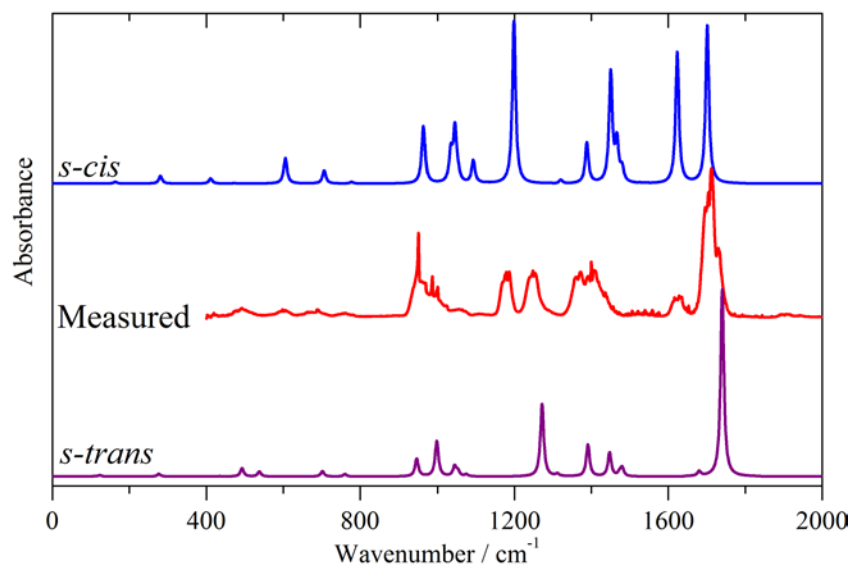
Figure 6. Comparison of (a) measured and calculated infrared spectra of 3-butene-2-one. Bottom: *s-trans* conformer (**1**), middle: measured spectrum, top: *s-cis* conformer (**2**). Note that the ordinate scale for the *s-cis* conformer is ×2 that of the *s-trans* conformer.
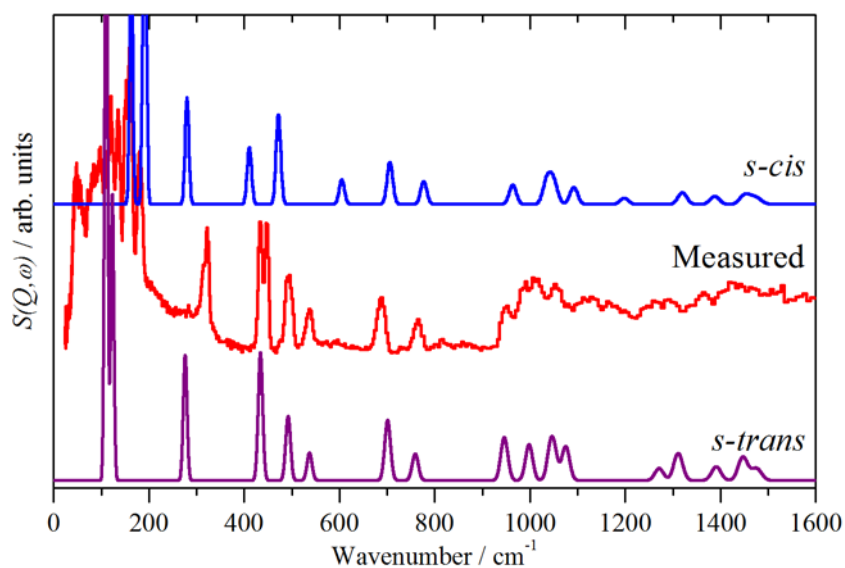

Figure 7. Comparison of (a) measured and calculated INS spectra of 3-butene-2-one. Bottom: *s-trans* conformer (**1**), middle: measured spectrum, top: *s-cis* conformer (**2**). Fundamentals only

13

Table 3. Measured and calculated vibrational transition energies for the conformers of 3-butene-2-one.

Experimental /cm^{-1}		DFT s-trans conformer		DFT s-cis conformer‡			Assignment
Infrared (gas phase RT)†	INS (solid 20 K)	/cm^{-1}	Infrared intensity / km mol^{-1}	/cm^{-1}	Infrared intensity / km mol^{-1}	Symmetry	
		111	0.39	191	0.00	A″	C1 methyl torsion
		123	1.44	163	0.99	A″	C2–C3 torsion
	323	277	2.91	411	2.91	A′	C1–C2–C3 in-plane bend
	434/438	435	0.31	473	0.25	A″	C=O out-of-plane bend
494 w / 598 w*	494	492	9.10	605	14.66	A′	C=O in-plane bend
	537	535	5.38	281	4.29	A′	C2–C3–C4 in-plane bend
689 w	688	702	5.86	706	7.53	A″	=CH$_2$ twist
759 w	764	760	2.63	778	0.91	A′	In-phase C–C stretches (C1–C2, C2–C3)
950 s	946	947	19.80	1093	13.18	A′	=CH$_2$ rock
985	994	998	39.42	1035	17.11	A″	=CH$_2$ wag

1002 w	1010	1044	10.67	1045	30.80	A″	C3–H out-of-plane bend
	1056	1053	5.85	1053	3.91	A″	Methyl rock
1058 w		1075	2.23	<mark>964</mark>	32.83	A′	Methyl rock
1182 s / 1244 s		1272	81.08	1199	93.64	A′	Out-of-phase C–C stretches (C1–C2, C2–C3)
		1311	2.55	1321	2.18	A′	C3–H in-plane bend
1367 m		1391	35.83	1388	23.22	A′	Symmetric methyl HCH bend
1406 s /		1447	26.69	1450	63.29	A′	=CH$_2$ scissors
		1473	3.80	1466	22.81	A′	Asymmetric methyl HCH bend
		1480	9.41	1480	7.68	A″	Asymmetric methyl HCH bend
1626 m		1680	5.08	1623	75.45	A′	C=C stretch
1713 vs		1740	208.86	1701	90.87	A′	C=O stretch
2941 w		3037	3.33	3000	2.55	A′	Symmetric methyl stretch
		3091	6.67	3053	7.57	A″	Asymmetric methyl stretch
2976 w		3142	4.86	<mark>3100</mark>	6.00	A′	Asymmetric methyl stretch
		3143	7.27	<mark>3096</mark>	7.47	A′	=CH$_2$ symmetric stretch
3018 w		3165	2.28	3108	13.29	A′	C3–H stretch

3104 w	3223	6.38	3178	2.33	*A′*	=CH$_2$ asymmetric stretch

†s = strong; m = medium; w = weak; sh = shoulder; br = broad; v = very

‡Modes where the order of the transition energies differs between the conformers are highlighted.

*s-cis modes are given are italics.

3.3 2-Butanone

Conformational isomerism in 2-butanone has been extensively discussed [30-35] with both structural [30-32] and spectroscopic studies finding little evidence for the presence of a *gauche* conformer. The conclusion from the experimental studies was that at room temperature, ~95% of the population was the *all-trans* conformer. Computational studies confirm this as shown in Figure 8. In addition to the *all-trans* conformer, there are two metastable *gauche* conformers ~4 kJ mol^{-1} higher in energy, however, the barriers between them and the ground state are very small, accounting for the small population. Because of the predominance of the *all-trans* conformer, this is the only one we consider here.
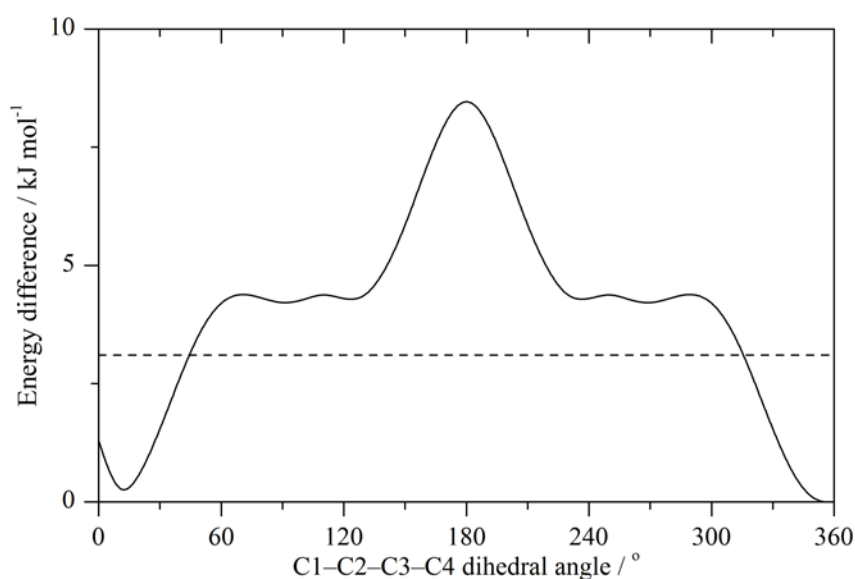

Figure 8. Potential energy scan around the C2–C3 bond of 2-butanone. The horizontal dashed line corresponds to kT = 373 K, the experimental reaction temperature.

Previous work has found the *all-trans* conformer with C_s symmetry to be the ground state, in our work, we found that a C_1 species with a slightly non-planar carbon skeleton was the lowest energy species. All attempts to impose C_s symmetry resulted in one imaginary mode corresponding to rotation about the C2–C3 bond. To test whether the C1 methyl group orientation was significant a potential energy scan as a function of orientation was carried out, see Figure 9. The orientation makes only ~1 kJ mol^{-1} difference, thus justifying our disregard of the effect of the methyl group orientation. The lowest energy structure had the methyl group in the position corresponding to the minima in Figure 9. We are unable to explain the disagreement with the literature results, despite having used a similar level of theory. Except for the imaginary mode, the transition energies for the C_s and C_1 structures are almost identical.
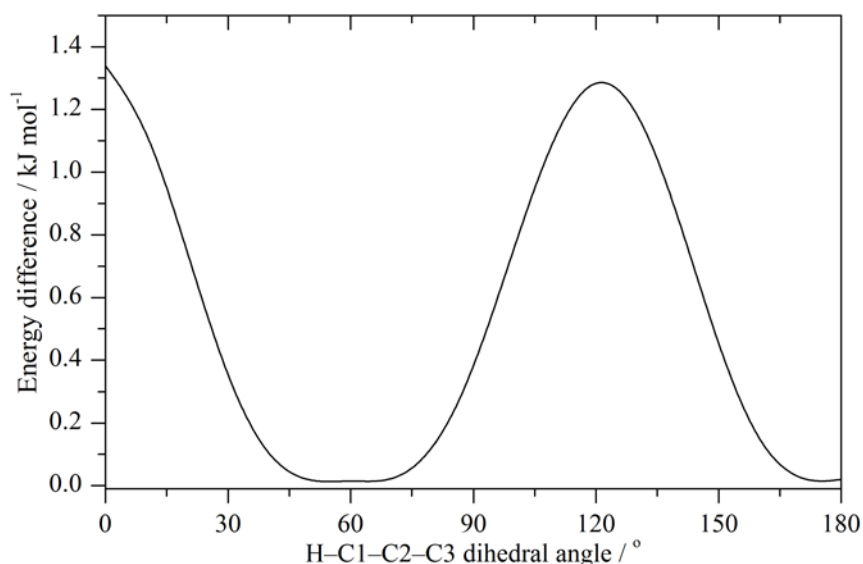
Figure 9. Potential energy scan of the C1 methyl group orientation in 2-butanone.

Column 5 of Table 1 gives the calculated structural data for *all-trans* 2-butanone and compares it with the structure as determined by electron diffraction [31] and the rotational constants from microwave spectroscopy [32]. The observed and calculated transition energies are given in Table 4 and comparisons of the infrared and INS spectra in Figures 10 and 11 respectively. From both the infrared and INS spectra there is no evidence for a second conformer, in agreement with previous work that indicates that there is less than 5% of the *gauche* conformers present. The crystal structure of 2-butanone is not known, however, from the splitting of the C4 methyl torsion band at 228 and 236 cm^{-1} and the width of the C1 methyl torsion band at 149 cm^{-1} in the INS spectrum, it is clear that there must be at least two molecules in the unit cell.

Table 4. Measured and calculated vibrational energies with assignments for *all-trans* 2-butanone.

Experimental /cm^{-1}		DFT		Assignment
Infrared (gas phase 323 K)†	INS (solid 20 K)	/ cm^{-1}	Infrared intensity / km mol^{-1}	
	72 vs	25	0.06	C2–C3 torsion
	149 s,br	103	0.14	C1 methyl torsion
	239/238 s	200	0.18	C4 methyl torsion
	264 s	247	5.33	C2–C3–C4 bend
	410 s	402	3.66	C1–C2–C3 bend
	447 sh/461 m	474	0.17	C=O out-of-plane bend
	591 w	588	8.20	C=O in-plane bend
	739 w	755	2.91	Methylene rock
	769 w	760	3.59	In-phase C–C stretch (C1–C2, C2–C3)
942 m	940 w	940	14.98	Methyl rock (C1)
		955	3.17	Methyl rock (C1)

	997 w	1000	2.01	C3–C4 stretch
1090 w	1090 w	1107	1.74	Methyl rock (C4)
	1110 w	1135	0.23	Methyl rock (C4)
1170 s	1175 w	1188	70.34	Out-of-phase C–C stretch (C1–C2, C2–C3)
	1261 w	1287	0.00	Methylene twist
		1371	13.00	Methylene wag
1370 s		1389	40.40	Sym. methyl HCH bend (C1)
		1418	5.34	Sym. methyl HCH bend (C4)
	1403 w,br	1452	4.77	Methylene scissors
1457 m		1468	23.10	Asym. methyl HCH bend (C1)
		1479	9.02	Asym. methyl HCH bend (C1)
	1456 w	1493	7.71	Asym. methyl HCH bend (C4)
		1500	7.95	Asym. methyl HCH bend (C4)

1742 vs	1780	164.79	C=O stretch
2917 w	3009	17.00	Sym. methylene stretch
	3030	6.70	Asym. methylene stretch
	3031	9.15	Sym. methyl stretch (C1)
2950 w	3042	22.97	Sym. methyl stretch (C4)
	3083	9.40	Asym. methyl stretch (C1)
	3104	20.81	Asym. methyl stretch (C4)
2992 w	3111	22.23	Asym. methyl stretch (C4)
	3138	9.94	Asym. methyl stretch (C1)

†s = strong; m = medium; w = weak; sh = shoulder; br = broad; v = very; sym = symmetric; asym = antisymmetric
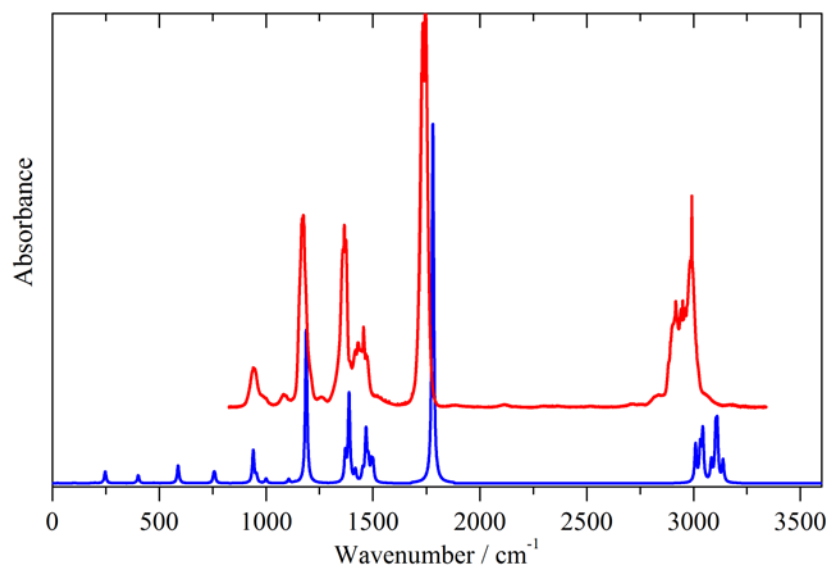
Figure 10. Comparison of measured (red, upper) and calculated (blue, lower) infrared spectra of 2-butanone (**4**).
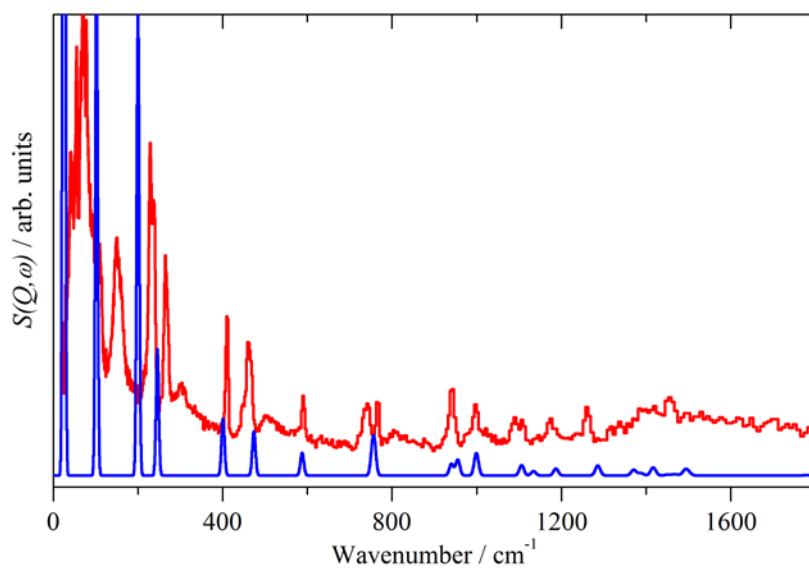

Figure 11. Comparison of measured (red, upper) and calculated (blue, lower) INS spectra of 2-butanone (**4**). Fundamentals only.

3.4   2-Butanol

2-Butanol has attracted attention [36-40] because it is the simplest inherently chiral alcohol. It has also been considered as a model for the O–C–C–C moiety found in C-glycosides. In addition, it has a rich conformational chemistry because of the possibility of conformational isomerism about the C2–C3 and C–O bonds. For the experimental studies, racemic 2-butanol was used, for the computational studies we have arbitrarily chosen (*R*)-2-butanol.

The results of a 2D potential energy scan about the C2–C3 and C–O bonds are shown in Figure 12 and cuts where the minima occur in Figure 13. There are nine minima corresponding to the conformations shown in Figure 14. We find that the three lowest minima are the (Tt), (Tg$^-$) and (Tg$^+$) conformations, although other authors [39,40] find a *gauche* conformation as the third lowest. However, the energy differences are small and depend on the level of theory used. In our case, the six higher conformations are all *gauche* conformers and account for less than 25% of the population at room temperature, thus only the three lowest energy conformers will be considered further. Table 5 lists the calculated structural parameters
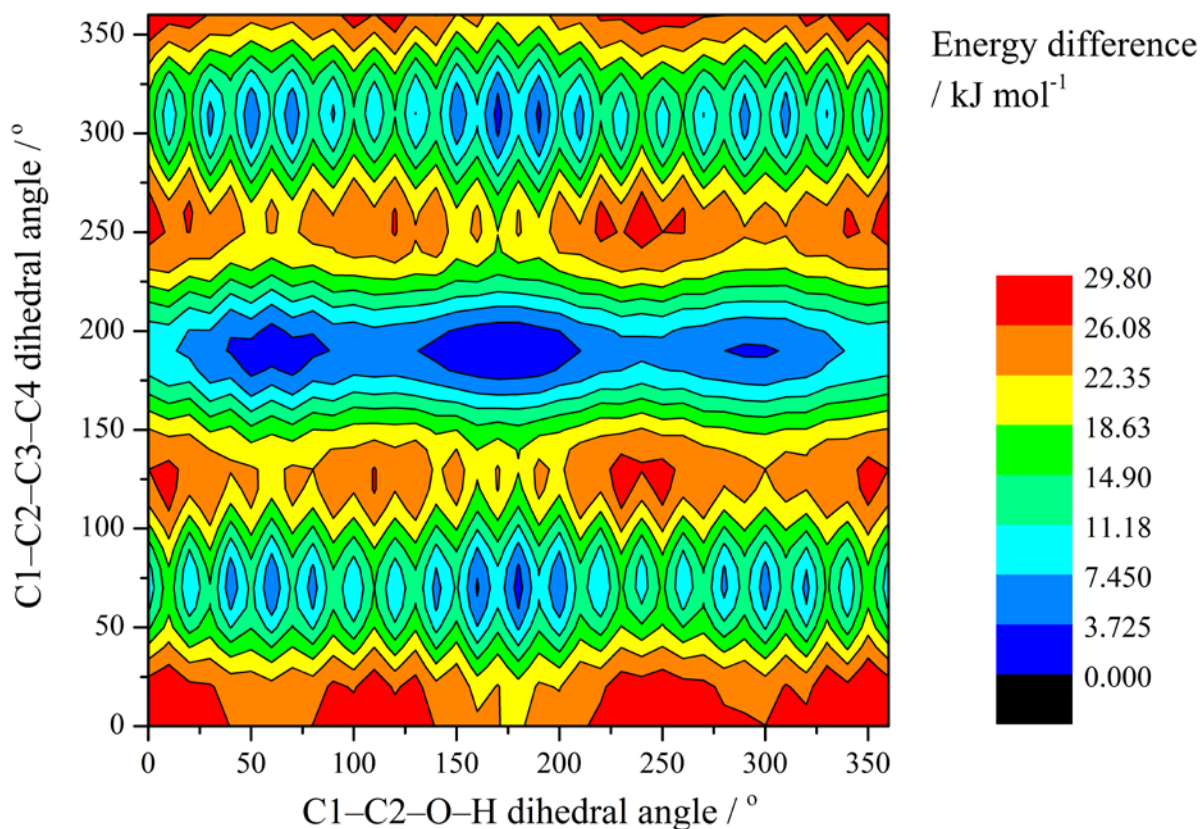

Figure 12. Potential energy surface for 2-butanol as a function of rotation about the C2–C3 and C2–O bonds.
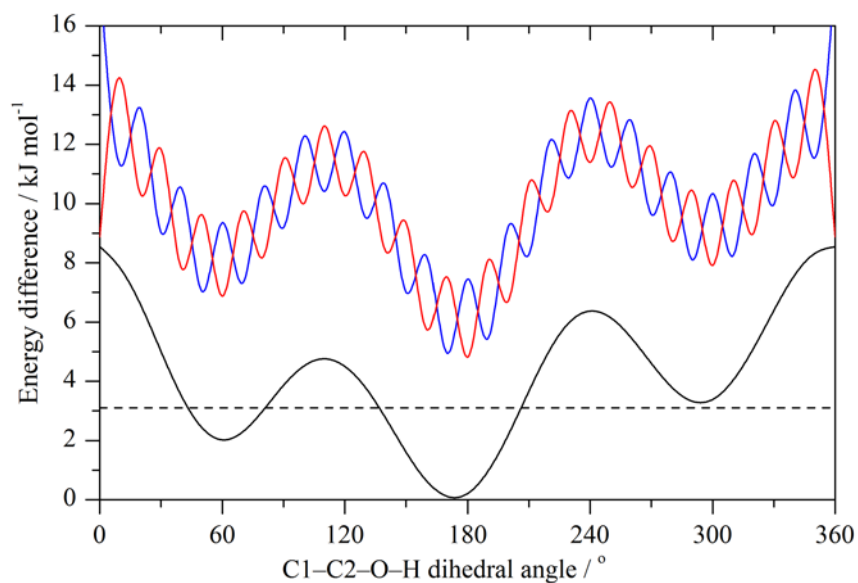
Figure 13. Cuts through the surface shown in Figure 12 at: ∠C1–C2–C3–C4 = 190° (black trace), = 70° (red trace), = 310° (blue trace).
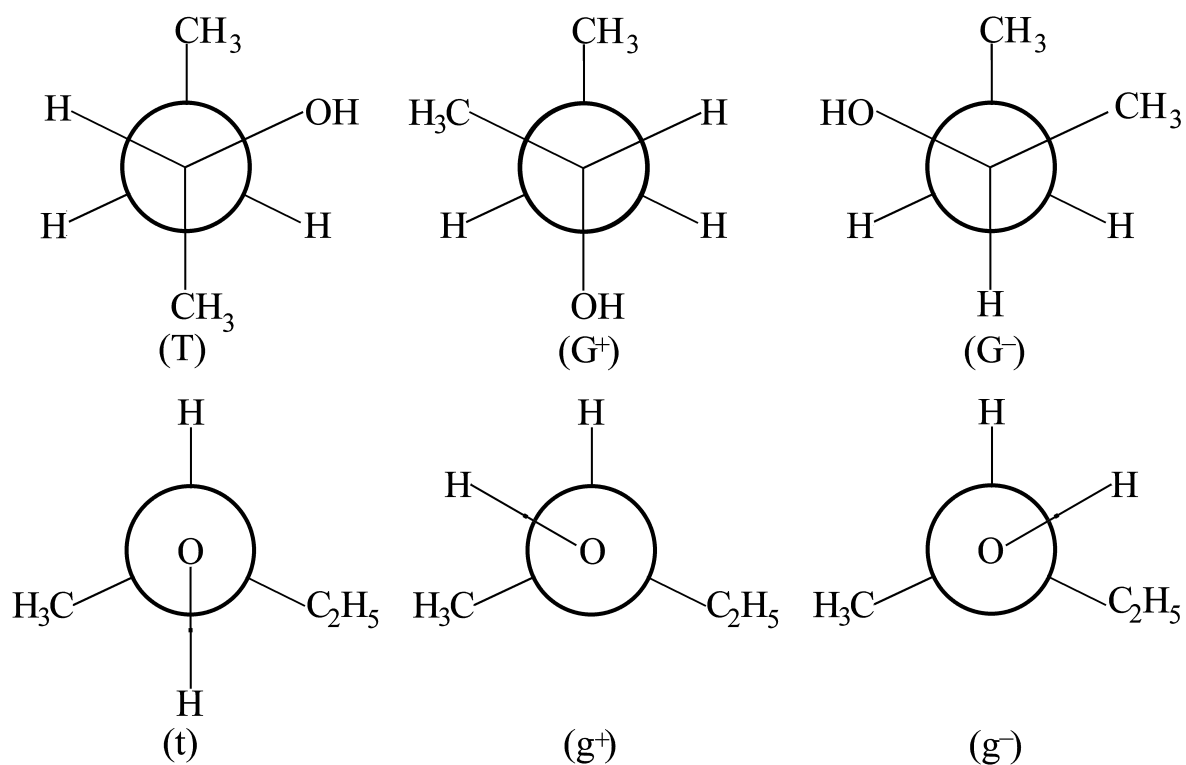

Figure 14. Conformers of (*R*)-2-butanol. Top row: as viewed along the C2–C3 bond, bottom row: as viewed along the C2–O bond.

Table 5. Selected structural parameters for the three lowest energy conformers of (*R*)-2-butanol (**5** - **7**).

	(Tt) conformer C_1 (**5**)	(Tg⁻) conformer C_1 (**6**)	(Tg⁺) conformer C_1 (**7**)
Bond distance / Å			
C1–C2	1.524	1.519	1.524
C2–C3	1.524	1.530	1.530
C3–C4	1.527	1.528	1.527
C2–O	1.436	1.435	1.434
C1–H	1.092, 2 × 1.091	1.089, 1.091 1.090	1.091,1.094 1.090
C2–H	1.099	1.099	1.093
C3–H	1.094, 1.093	1.093, 1.093	1.096, 1.094
C4–H	1.091, 1.092, 1.089	1.090, 2 × 1.092	1.090, 1.094, 1.092
O–H	0.962	0.961	0.963
Bond angle / °			
C1–C2–C3	112.5	112.4	112.5
C2–C3–C4	113.8	114.1	113.8
C1–C2–O	111.0	106.3	110.9)
C3–C2–O	106.9	111.9	111.6
Dihedral angle / °			
C1–C2–C3–C4	175.8	177.8	175.0

C1–C2(–O)–C3	-122.1	-119.5	-125.5
Rotational constants / MHz			
A	8074	8097	7943
B	3438	3418	3418
C	2665	2645	2654

For 2-butanol, we restrict the discussion to the region <2800 cm^{-1} since the similarity of the transition energies of the aliphatic groups means that the aliphatic C–H stretch region is highly congested and not useful for reaction monitoring. The experimental spectra and the calculated spectra of the three conformers are shown in Figures 15 (infrared) and 16 (INS) respectively and listed in Table 6. The infrared spectra show some variations with conformer and the relative intensities of the experimental bands would suggest the presence of all three conformers. In contrast, the INS spectra show relatively little difference between the conformers. Surprisingly, the O–H deformation modes give weak bands at the calculated frequencies, suggesting that the solid is not strongly hydrogen bonded and justifying our assumption of weak intermolecular interactions. The broad, featureless nature of the lattice modes would indicate that a glass is formed rather than a crystalline solid.
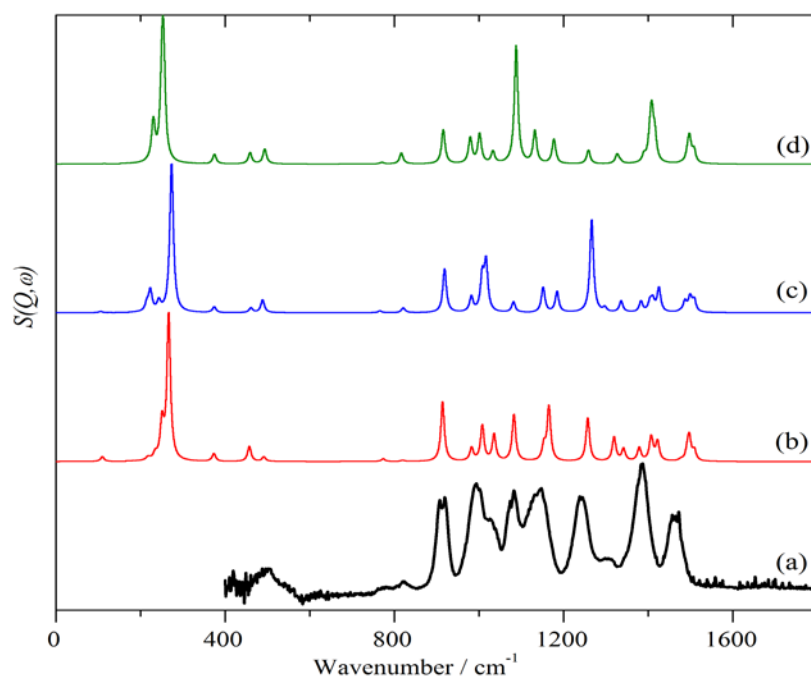

Figure 15. Comparison of (a) measured and calculated infrared spectra of 2-butanol, (b) (Tt) conformer (**5**), (c) (Tg$^-$) conformer (**6**) and (d) (Tg$^+$) conformer (**7**).
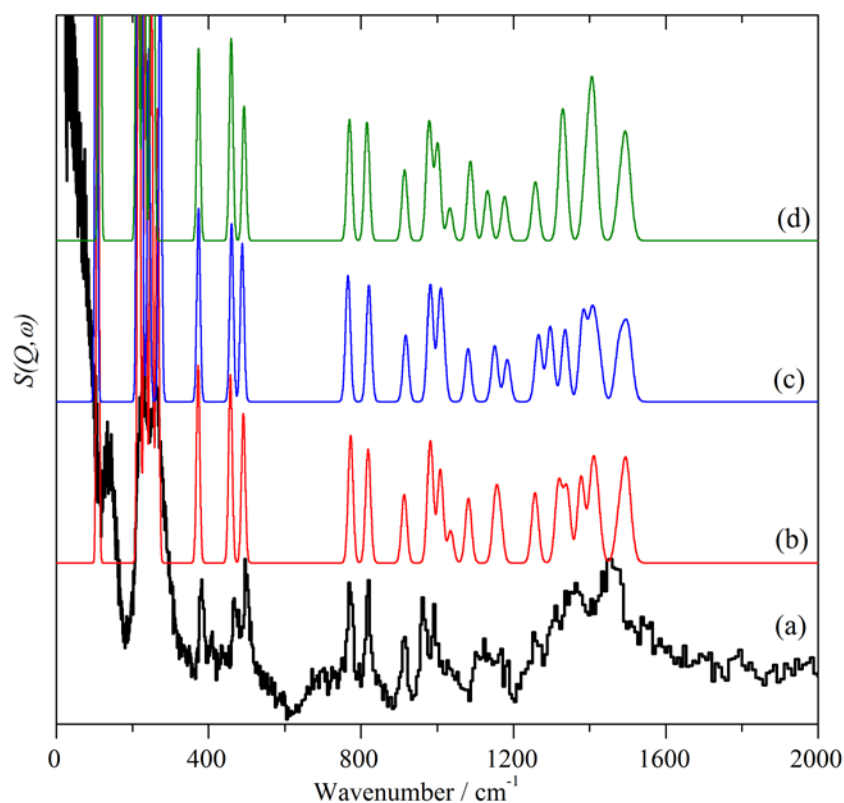
Figure 16. Comparison of (a) measured and calculated INS spectra of 2-butanol, (b) (Tt) conformer (**5**), (c) (Tg$^-$) conformer (**6**) and (d) (Tg$^+$) conformer (**7**). Fundamentals only.

4.   Conclusions

The DFT calculations reported here have allowed complete assignments for the four molecules of interest. These are generally in agreement with the largely empirical assignments in the literature. However, the certainty that is provided by our DFT results mean that the bands chosen for the reaction study reported in the main paper can be confidently assigned to the species of interest.

Acknowledgements

Table 6. Measured and calculated vibrational energies with assignments for three lowest energy conformers of (*R*)-2-butanol (**5** - **7**).

Experimental / cm^{-1}		DFT / cm^{-1}						
		(Tt) conformer C_1 (**5**)		(Tg$^-$) conformer C_1 (**6**)		(Tg$^+$) conformer C_1 (**7**)		
Infrared (gas phase 323 K)†	INS (solid 20 K)	/ cm^{-1}	Infrared intensity / km mol^{-1}	/ cm^{-1}	Infrared intensity / km mol^{-1}	/ cm^{-1}	Infrared intensity / km mol^{-1}	Assignment
	135 s	110	2.61	106	0.78	115	0.21	C2–C3 torsion
	230 s	218	1.65	215	4.52	214	0.21	C4 torsion
		235	3.18	223	12.56	230	21.75	C2–C3–C4 bend
	261 s	251	20.09	243	5.81	255	48.32	C1 torsion
		267	80.14	273	90.06	251	41.05	O–H out-of-plane bend
	383 m	373	4.41	374	3.52	375	5.25	C1–C2–C3 bend
	468 w	457	8.23	461	2.83	459	6.04	Out-of- plane skeletal deformation
501 w,br	501 m	491	2.41	489	7.78	494	7.97	Out-of- plane skeletal deformation
771 vw	773 m	773	1.48	766	1.05	771	0.82	Methylene rock

821 vw	823 m	820	0.61	821	2.85	817	5.95	Methyl rock
913 m	919 m	914	32.66	919	26.21	916	18.47	Methyl rock
	965 m	983	7.06	982	8.96	979	13.97	Methyl rock
994 m	994 w	1008	19.38	1008	20.68	1002	15.86	Methyl rock
1027 sh		1036	14.63	1016	29.15	1033	6.31	C3–C4 stretch
1081 m		1083	25.58	1081	6.21	1087	64.08	Out-of-phase C–C stretch (C1–C2, C2–C3)
1145 m		1154	7.96	1152	15.18			C–O stretch
	1138 w, br	1166	29.77	1185	12.43			In-phase C–C stretch (C1–C2, C2–C3)
1241 m	1266 w	1257	23.71	1267	56.00	1259	7.49	O–H in-plane bend
1308 vw	1313 w	1320	13.19	1297	2.57	1334	1.15	Methylene twist
		1342	6.62	1336	6.75	1390	3.69	Methylene wag
	1364 w	1379	7.29	1383	6.52	1326	5.07	C2–H bend
1385 m		1407	11.40	1404	5.88	1404	9.36	Sym. methyl bend (C1)
		1410	2.52	1411	6.70	1415	13.48	Sym. methyl bend (C4)
		1422	10.49	1425	14.47	1408	24.68	C2–H bend
		1477	0.74	1475	0.54	1479	0.29	Methylene scissors

	1494	4.50	1498	6.30	1493	4.12	Asym. methyl bend (C1)
1462 m	1497	9.75	1498	6.31	1496	0.18	Asym. methyl bend (C4)
	1498	2.65	1501	2.98	1497	12.72	Asym. methyl bend (C1)
1467 m	1509	5.51	1509	7.09	1508	6.70	Asym. methyl bend (C4)

†s = strong; m = medium; w = weak; sh = shoulder; br = broad; v = very; sym = symmetric; asym = antisymmetric

References

[1] Z. Yin, L. Lin and D. Ma, *Catal. Sci. Technol.* 4 (2014) 4116.

[2] Y. Nie, L. Li and Z. Wei, *Chem. Soc. Rev.* 44 (2015) 2168.

[3] D.R. Kennedy, G. Webb, S.D. Jackson and D. Lennon, *Appl. Catal. A: Gen.* 259 (2004) 109.

[4] K. Möbus, E. Grünewald, S. Wieland, S.F. Parker and P.W. Albers, *Journal of Catalysis* 311 (2014) 153-160.

[5] P.W. Albers, K. Möbus, S.D. Wieland and S.F. Parker, *Physical Chemistry Chemical Physics,* 17 (2015) 5274–5278.

[6] E. Opara, D. T. Lundie, T. Lear, I. W. Sutherland, S. F. Parker and D. Lennon, *Phys. Chem. Chem. Phys.* 6 (2004) 5588.

[7] A. McFarlane, L. McMillan, I. P. Silverwood, N. G. Hamilton, D. Siegel, S. F. Parker, D. T. Lundie and D. Lennon, *Catal. Today* 155 (2010) 206.

[8] S.F. Parker, D. Siegel, N.G. Hamilton, J. Kapitán, L. Hecht and D. Lennon, *J. Phys. Chem. A* 116 (2012) 333–346.

[9] P. C. H. Mitchell, S. F. Parker, A. J. Ramirez-Cuesta, J. Tomkinson, *Vibrational Spectroscopy With Neutrons, With Applications in Chemistry, Biology, Materials Science and Catalysis*, World Scientific: Singapore, **2005**.

[10] A. Navarro, J.J. López-González, G.J. Kearley, J. Tomkinson, S.F. Parker and D.S. Sivia, *Chem. Phys*. 200 (1995) 395-403.

[11] A. Navarro, M. Fernández-Gómez, J.J. López-González and M. Paz Fernández-Liencres, *J. Phys. Chem. A* 103 (1999) 5833-5840.

[12] S.F. Parker, K.P.J. Williams, D. Steele and H. Herman, *Phys. Chem. Chem. Phys.* 5 (2003) 1508 - 1514.

[13] D. G. Allis, H. Prinzbach and B. S. Hudson, *Chem. Phys. Lett.* 386 (2004) 356–363.

[14] A. Pawlukojć, J. Leciejewicz, A.J. Ramirez-Cuesta and J. Nowicka-Scheibe, *Spectrochim. Acta A* 61 (2005) 2474–2481.

[15] S.F. Parker, F. Fernandez-Alonso, A.J. Ramirez-Cuesta, J. Tomkinson, S. Rudic, R.S. Pinna, G. Gorini and J. Fernández Castañon, *Journal of Physics Conference Series*, 554 (2014) 012003.

[16] http://www.isis.stfc.ac.uk/

[17] M.J. Frisch, G.W. Trucks, H.B. Schlegel, G.E. Scuseria, M.A. Robb, J.R. Cheeseman, J.A. Montgomery Jr, T. Vreven, K.N. Kudin, J.C. Burant, J.M. Millam, S.S. Iyengar,

J. Tomasi, V. Barone, B.Mennucci, M. Cossi, G. Scalmani, N. Rega, G.A. Petersson, H. Nakatsuji, M. Hada, M. Ehara, K. Toyota, R. Fukuda, J. Hasegawa, M. Ishida, T. Nakajima, Y. Honda, O. Kitao, H. Nakai, M. Klene, X. Li, J.E. Knox, H.P. Hratchian, J.B. Cross, C. Adamo, J. Jaramillo, R. Gomperts, R.E. Stratmann, O. Yazyev, A.J. Austin, R. Cammi, C. Pomelli, J.W. Ochterski, P.Y. Ayala, K. Morokuma, G.A. Voth, P. Salvador, J.J. Dannenberg, V.G. Zakrzewski, S. Dapprich, A.D. Daniels, M.C. Strain, O. Farkas, D.K. Malick, A.D. Rabuck, K. Raghavachari, J.B. Foresman, J.V. Ortiz, Q. Cui, A.G. Baboul, S. Clifford, J. Cioslowski, B.B. Stefanov, G. Liu, A. Liashenko, P. Piskorz, I. Komaromi, R.L. Martin, D.J. Fox, T. Keith, M.A. Al- Laham, C.Y. Peng, A. Nanayakkara, M. Challacombe, P.M.W. Gill, B. Johnson,W. Chen, M.W. Wong, C. Gonzalez, J.A. Pople, *Gaussian 03*, Revision B.05, Gaussian, Inc.: Pittsburgh, PA, **2003**.

[18] A. J. Ramirez-Cuesta, *Comput. Phys. Commun.* **2004**, *157*, 226.

[19] G.A. Crowder, *Spectrochim Acta* 19A (1963) 1885-1889.

[20] D. Pierotti, S.C. Wofsy and D. Jacob, *J. Geophys. Res.* 95 (1990) 1871.

[21] P.D. Foster, V.M. Rao and R.F. Curl Jr., *J. Chem. Phys.* 43 (1965) 1064.

[22] A.C. Fantoni, W. Caminati and R. Meyer, *Chem. Phys. Lett.* 133 (1987) 27.

[23] J. De Smedt, F. Vanhouteghem, C. Van Alsenoy and H.J. Geise, *J. Mol. Struct. 19*5 (1989) 227.

[24] D.S. Wilcox, A.J. Shirar, O.L. Williams, B.C. Dian, *Chem. Phys. Lett.* 508 (2011) 10.

[25] K. Noack and R.N. Jones, *Can. J. Chem.* 39 (1961) 2225.

[26] A.J. Bowles, W.O. George, W.F. Maddams, *J. Chem. Soc. B* (1969) 810.

[27] J.R. Durig and T.S. Little, *J. Chem. Phys. 7*5 (1981) 3660.

[28] H.J. Oelichmann, D. Bougeard and B. Schrader, *J. Mol. Struct.* 77 (1981) 179.

[29] K. Sankaran and Y.-P. Lee, *J. Phys. Chem. A* 106 (2002) 1190.

[30] C. Romers and J.E.G. Creutzberg, *Recueil des Travaux Chimiques des Pays-Bas* 75 (1956) 331-345.

[31] M. Abe, K. Kuchitsu and T. Shimanouchi, *J. Mol. Struct.* 4 (1969) 245.

[32] L. Pierce, C.K. Chang, M. Hayashi and R. Nelson, *J. Mol. Spectrosc.* 5 (1969) 449-457.

[33] T. Shimanouchi, Y. Abe and M. Mikami, *Spectrochim. Acta* 24A (1968) 1037–1053.

[34] J.R. Durig, F.S. Feng, A. Wang and H.V. Phan, *Can. J. Chem.* 69 (1991) 1827.

[35] H. Zhong, E. L. Stewart, M. Kontoyianni and J.P. Bowen, *J. Chem. Theory Comput.* 1 (2005) 230-238.

[36] A.K. King and B.J. Howard, *J. Mol. Spectrosc.* 205 (2001) 38–42.

[37] A.K. King and B.J. Howard, *J. Mol. Spectrosc.* 257 (2009) 205–212.

[38] H. Hagemann, J. Mareda, C. Chiancone, H. Bill, *J. Mol. Struct.* 410–1 (1997) 357-360.

[39] F. Wang and P.L. Polavarapu, *J. Phys. Chem. A* 104 (2000) 10683–10687.

[40] S. Shin, M. Nakata and Y. Hamada, *J. Phys. Chem. A* 110 (2006) 2122–2129.